Water Research 185 (2020) 116261

Contents lists available at ScienceDirect

Water Research

journal homepage: www.elsevier.com/locate/watres

# Quantification of *nosZ* genes and transcripts in activated sludge microbiomes with novel group-specific qPCR methods validated with metagenomic analyses

Daehyun D. Kim[a], Doyoung Park[a], Hyun Yoon[a,b], Taeho Yun[a], Min Joon Song[a], Sukhwan Yoon[a,*]

[a] Department of Civil and Environmental Engineering, Korea Advanced Institute of Science and Technology (KAIST), Daejeon 350-701, Korea
[b] Department of Civil and Environmental Engineering, Cornell University, Ithaca, NY, 14853, USA

ARTICLE INFO

*Article history:*
Received 10 April 2020
Revised 14 July 2020
Accepted 1 August 2020
Available online 5 August 2020

*Keywords:*
Nitrous oxide reductase
Quantitative PCR
Reverse transcription quantitative PCR
Activated sludge
Metagenomics

ABSTRACT

Substantial $N_2O$ emission results from activated sludge nitrogen removal processes. $N_2O$-reducing organisms possessing NosZ-type $N_2O$ reductases have been recognized to play crucial roles in suppressing emission of $N_2O$ produced in anoxic activated sludge via denitrification; however, which of the diverse *nosZ*-possessing organisms function as the major $N_2O$ sink *in situ* remains largely unknown. Here, *nosZ* genes and transcripts in wastewater microbiomes were analyzed with the group-specific qPCR assays designed *de novo* combining culture-based and computational approaches. A sewage sample was enriched in a batch reactor fed continuous stream of $N_2$ containing 20-10,000 ppmv $N_2O$ with excess amount (10 mM) of acetate as the source of carbon and electrons, where 14 genera of potential $N_2O$-reducers were identified. All available amino acid sequences of NosZ affiliated to these taxa were grouped into five subgroups (two clade I and three clade II groups), and primers/probe sets exclusively and comprehensively targeting the subgroups were designed and validated with *in silico* PCR. Four distinct activated sludge samples from three different wastewater treatment plants in Korea were analyzed with the qPCR assays and the results were validated with the shotgun metagenome analysis results. With these group-specific qPCR assays, the *nosZ* genes and transcripts of six additional activated sludge samples were analyzed and the results of the analyses clearly indicated the dominance of two clade II *nosZ* subgroups (*Flavobacterium*-like and *Dechloromonas*-like) among both *nosZ* gene and transcript pools.



## 1. Introduction

Nitrous oxide ($N_2O$) is one of the three major greenhouse gases with the largest contributions to global warming, along with $CO_2$ and $CH_4$ (Ciais et al., 2013). Although the contribution of $N_2O$ is estimated to be only ~6% of the net greenhouse gas emissions in terms of $CO_2$eq, which is far less than those of $CO_2$ and $CH_4$, eliminating one molecule of $N_2O$ from the atmosphere has the same merit as removing ~300 molecule of $CO_2$ due to its high global warming potential. Further, $N_2O$ has also been the most consequential ozone depletion agent (Portmann et al., 2012; Ravishankara et al., 2009). Thus, global efforts to curb the increase in atmospheric $N_2O$ concentration are necessitated for sustainable future. As sources and sinks of $N_2O$ in the environments are predominantly biological, an improved understanding of the microbial guilds and biochemical reactions involved in production or consumption of $N_2O$ is a pre-requisite for devising strategies for its emission mitigation (Ciais et al., 2013).

Particularly, the biological $N_2O$ reduction mediated by Nos-type nitrous oxide reductases (NosZ) has recently attracted immense scientific attention as the sole sink of $N_2O$ on the Earth's surface at non-elevated temperature (Frutos et al., 2018; Hallin et al., 2017; Suenaga et al., 2019; Thomson et al., 2012). This reaction had been, for long, known merely as one of the stepwise reactions constituting the denitrification pathway (Yoon et al., 2019b; Zumft, 1997). Only recently has the $N_2O$-to-$N_2$ reduction been recognized as an independent energy-conserving reaction, as diverse organisms possessing either conventional clade I and newly-discovered clade II *nosZ* were found to be capable of growth with $N_2O$ as the sole electron acceptor (Conthe et al., 2018b; Sanford et al., 2012; Suenaga et al., 2019; Yoon et al., 2016). Several independent research groups have reported difference between clade I and clade

* Corresponding author.
*E-mail address:* syoon80@kaist.ac.kr (S. Yoon).

https://doi.org/10.1016/j.watres.2020.116261
0043-1354/

II *nosZ*-possessing organisms in terms of their biokinetic properties (Domeignoz-Horta1 et al., 2015; Jones et al., 2014; Suenaga et al., 2019; Suenaga et al., 2018; Yoon et al., 2016). More specifically, the organisms with *nosZ* closely affiliated to *Dechloromonas* spp. have been reported with particularly low whole-cell Michaelis-Menton half saturation constants, suggesting that this group of organisms may be involved in *in situ* consumption of low-concentration $N_2O$ produced via diverse biotic and abiotic processes. The microbial community developed in the laboratory-scale biofilter treating 100 ppmv $N_2O$ included the clade II $N_2O$ reducers *Flavobacterium* spp. as the most abundant *nosZ*-carrying organisms, also supporting the significance of clade II $N_2O$ as an important $N_2O$ sink (Yoon et al., 2019a; Yoon et al., 2017).

Nitrogen turnover in wastewater treatment plants (WWTPs) occurs at a much shorter time scale than other major $N_2O$ sources, e.g., agricultural soils, and thus, anoxic activated sludge is the environment where the most rapid NosZ-mediated $N_2O$ reduction take place on an everyday basis (Law et al., 2012). Therefore, WWTP has been one of the environmental systems most intensely investigated for improved understanding of NosZ-mediated $N_2O$ reduction and its role in suppressing emission of $N_2O$ produced *in situ* via denitrification (Boonnorat et al., 2018; Conthe et al.; Conthe et al., 2018b; Song et al., 2015; Vieira et al., 2019). Many of these recent investigations endeavored to correlate $N_2O$ reduction activities in activated sludge reactors to gene/transcript abundances of the two distinct *nosZ* clades. The analytical methods that have been most frequently used for such clade-specific quantification of *nosZ* are SYBR Green based quantitative polymerase chain reactions (qPCR) separately targeting clade I (1840F: 5'-CGCRACGGCAASAAGGTSMSSGT-3'/ 2090R: 5'-CAKRTGCAKSGCRTGGCAGAA-3') and clade II *nosZ* (nosZ-II-F: 5'-CTIGGICCIYTKCAYAC-3' / nosZ-II-R: 5'-SKSACCTTIITTRCCITYICG-3') (Henry et al., 2006; Jones et al., 2014). Often, these qPCR assays lack the level of accuracy needed for finding credible answers to even the simplest ecological questions regarding clade I vs clade II *nosZ* competition, presumably due, in part, to their low amplification efficiencies (Conthe et al., 2018b; Di et al., 2014; Stoliker et al., 2016). Further, growing evidence that clade distinction may not be sufficiently specific for understanding the competition and niche specialization of different $N_2O$-reducing organisms have called for new quantification methods with narrower target groups (Gabarró et al., 2013; Suenaga et al., 2019; Yoon et al., 2019a; Yoon et al., 2017). In this study, we have developed TaqMan-based qPCR targeting four groups (two clade I *nosZ* groups and two clade II *nosZ* groups) of *nosZ* with amplification efficiency above 90% and verified their improved predictability by comparing the quantification data with the results of shotgun metagenome analyses. Anoxic activated sludge samples from anoxic tanks of six conventional wastewater treatment plants in Korea with A2O (anaerobic-anoxic-oxic) configuration were then analyzed with these novel qPCR assays. Without exception, clade II domination of *nosZ* gene and transcript pools was verified in these activated sludge samples.

## 2. Materials and methods

### 2.1. Sample collection

The wastewater inoculum for the $N_2O$ enrichment experiments were grab-sampled from the anoxic section of the activated sludge tank at Daejeon municipal WWTP (36º23'5" N 127º24'28" E) in September 2016 (denoted as Daejeon1). The activated sludge samples for validation of the qPCR assays were collected at the same WWTP (Daejeon2) in February 2019 and two other activated sludge WWTPs located in Gwangju and Gapyeong (35°09′22.4"N 126°49′51.6"E and 37°49′00.1"N 127°31′13.0"E, respectively) in January and February 2019, respectively. Activated sludge samples from anoxic tanks of six other A2O (anaerobic/anoxic/oxic) WWTPs were then collected for group-specific quantification of *nosZ* genes and transcripts with the developed qPCR assays (Fig. S1, Table S1). The selection criteria for the study sites were that the WWTPs were constructed and operated with A2O principle in accordance with the international standards (ISO 24516-4) and that their treatment capacities were larger than 10,000 $m^3$ $d^{-1}$. Each wastewater sample for analyses of DNA was collected in a 2-L polyethylene bottle filled up to the brim to minimize oxygen ingress. The samples for quantification of *nosZ* transcripts were immediately mixed with the same volume of methanol for RNA fixation (Binder and Liu, 1998). The sample bottles were immediately placed in a cooler and transported to the laboratory, where they were stored at -80°C until use.

### 2.2. Fed-batch enrichment of activated sludge samples and identification of active $N_2O$-hreducing groups

The initial attempts to design mutually exclusive group-specific qPCR primers/probe sets with the entire suite of *nosZ*-annotated genes from the NCBI RefSeq database were not successful, due to the high divergence of the *nosZ* genes and stringent design criteria for TaqMan-based qPCR necessitated to ensure high amplification efficiency and thus, reliable accuracy (e.g., presence of three conserved regions within a <400 bp stretch). Thus, as an alternative approach, $N_2O$-fed enrichments of the Daejeon1 sample were analyzed to narrow down the targeted *nosZ* sequences. As wastewater microbiomes share high similarity in their composition, using a single activated sludge sample was considered sufficient for designing *nosZ* qPCR primers/probe sets that can be universally applied to WWTPs of different geographical locations (Wu et al., 2019). A simple fed-batch bioreactor was constructed with a 500-mL glass bottle with a side port (Duran, Mainz, Germany) and a GL45 cap with three ports (Fig. S2). The GL45 ports were used as the inlet for $N_2O$-carrying gas, gas outlet from the bottle, and aqueous phase sampling port. The side port of the glass bottle was used for headspace sampling. The modified MR-1 medium was prepared by adding per 1 L of deionized water, 0.5 g NaCl, 0.23 g $KH_2PO_4$, 0.46 g $K_2HPO_4$, 0.026 g $NH_4Cl$, 1 ml of 1000X trace metal solution, and 1 mL of 1000X vitamin stock solution (Yoon et al., 2016). Sodium acetate was added as the source of carbon and electrons to an excess amount (10 mM). The choice of acetate, a non-fermentable substrate, as the sole source of carbon and electron was to prevent overgrowth of fermentative organisms (van den Berg et al., 2016). Acetate is oxidized via the citric acid cycle producing NADH, which is known to support proton translocation in organisms utilizing $N_2O$ as the terminal electron acceptor (Strohm et al., 2007). The reactor with 200-mL medium (40% of the total reactor volume) was flushed with 0 ppmv, 20 ppmv, 200 ppmv, or 10,000 ppmv $N_2O$ prepared in >99.999% $N_2$ gas (Samoh Specialty Gas, Daejeon, South Korea) for 30 hours before inoculation. After inoculating the medium with 2 mL of the Daejeon1 sample, the same gas was bubbled through the medium at the volumetric flowrate of 20 mL $min^{-1}$ to provide the sole electron acceptor $N_2O$ to the microbial culture and maintain the reactor at anoxic condition. The reactor operated with >99.999% $N_2$ gas served as the control to confirm that the microbial consortia were enriched with $N_2O$ as the electron acceptor and the contribution of $O_2$ contamination to microbial growth was kept minimal. The $N_2O$ concentration in the headspace of the reactor was monitored with a HP6890 Series gas chromatography fitted with an HP-PLOT/Q column and an electron capture detector (Agilent, Palo Alto, CA), with the injector, oven and detector temperatures set to 200, 85, and 250 ºC, respectively (Park et al., 2017). The $O_2$ concentration in the fed-batch reactor was monitored with a FireSting-$O_2$ oxygen meter (Pyroscience, Aachen, Germany); however, due to the relatively

high detection limit of the sensor (the gas phase concentration of ~0.1% v/v), complete absence of $O_2$ was not guaranteed.

The growth of bacterial population in the reactor was monitored with qPCR using TaqMan chemistry targeting the conserved region of eubacterial 16S rRNA genes. At each sampling time point, an 1.5-mL aliquot was collected from the aqueous phase of the reactor and DNA was extracted from the pellets using DNeasy Blood & Tissue Kit (Qiagen, Hilden, Germany) following the protocol provided by the manufacturer. Quantitative PCR was performed with the 1055f (5'-ATGGCTGTCGTCAGCT-3') / 1392r (5'-ACGGGCGGTGTGTAC-3') / Bac1115Probe (5'-CAACGAGCGCAACCC-3') primers and probe set using a QuantStudio3 Real Time PCR System (Thermo Fisher Scientific, Waltham, MA) (Ritalahti et al., 2006). Incubation was halted when the population of the enrichment reached a plateau, as indicated by three consecutive measurements without significant increase in the 16S rRNA gene counts. The reactor was dismantled and the aqueous phase was collected for microbial composition analysis. The hypervariable V6–8 region of the 16S rRNA gene was amplified with 926F: 5′-AAACTYAAAKGAATTGRCGG-3′ / 1392R: 5′-ACGGGCGGTGTGTRC-3′ primer set (Matsuki et al., 2002). MiSeq sequencing of the amplicons was outsourced to Macrogen Inc. (Seoul, Korea). The raw sequence reads were deposited in the NCBI short reads archive (SRA) database (accession: PRJNA552413) and were processed using the QIIME pipeline v 1.9.1. A detailed computational method is provided in the supplementary information.

### 2.3. Design of degenerate primers and probes for group-specific qPCR of nosZ genes

The genera assigned to the OTUs with the relative abundances higher than 0.3% in any of the reactor microbial communities were selected. All *nosZ* gene sequences and corresponding translated NosZ amino acid sequences belonging to the organisms affiliated to these genera were extracted from the Uniprot (www.uniprot.org) database (accessed in March 2017) (Table S2). The curated pools of *nosZ*/NosZ sequence data included, in total, 174 nucleotide sequences and the corresponding amino acid sequences from 14 distinct genera. Subsequently, a multiple sequence alignment was performed with these amino acid sequences, using MUSCLE algorithm with the parameters set to default values (Edgar, 2004). The NosZ phylogenetic tree was constructed using the neighbor-joining method in MEGA 7.0 with the bootstrap value set to 500 (Kumar et al., 2016). The *nosZ* gene sequences were clustered into five groups (NosZG1-5) according to the positions of the corresponding NosZ sequences in the phylogenetic tree, which consisted of five phylogenetically distinct subbranches.

For each *nosZ* group, a primers and probe set was designed using the PriMux software to comprehensively and exclusively target the *nosZ* gene sequences within the group (Hysom et al., 2012). The parameters were modified from the default values to obtain the optimal candidate degenerate oligonucleotide sequences for qPCR (length: 18-24 bp, amplicon size: 80-400 bp, $T_m$: 56-62°C for primers and 68 - 72°C for probes). Several candidate primers and probe sets were generated for each *nosZ* group, implementing the ***min***, ***max***, and ***combo*** algorithms of the Primux software. The performance of each candidate primers and probe set was predicted with *in silico* PCR performed with the simulate_PCR software against all genome sequences used for development of the primers and probe sets (Gardner and Slezak, 2014; Hysom et al., 2012). Coverage within the target *nosZ* group and mutual exclusivity across the groups were the two major criteria for assessment of the candidate primers and probe sets. The *in silico* PCR tests were also performed against the complete genomes of 50 bacterial strains lacking *nosZ* to preclude the possibility of unspecific amplification.

### 2.4. Construction of calibration curves for the designed primers and probe sets using model $N_2O$ reducer strains

For each *nosZ* group, a model organism was selected for construction of the qPCR calibration curve: *Pseudomonas stutzeri* DCP-Ps1 (NosZG1), *Acidovorax soli* DSM25157 (NosZG2), *Flavobacterium aquatile* LMG4008 (NosZG3), *Ignavibacterium album* JCM16511 (NosZG4), and *Dechloromonas aromatica* RCB (NosZG5). *Acidovorax soli* DSM25157 and *F. aquatile* LMG4008 were acquired from Korean Collection for Type Cultures and *I. album* JCM16511 from Japanese Collection of Microorganisms. The axenic batch cultures of these organisms were prepared as previously described in literature or using the media and incubation conditions specified by the distributors. The cells were harvested at $OD_{600nm}$ = 0.1 and the *nosZ* gene(s) in the DNA extracted from the cell pellets were amplified using the designed primers (Table S3). The calibration curve for each qPCR was constructed using ten-fold serial dilutions of pCR2.1™ vectors (Invitrogen, Carlsbad, CA) carrying the *nosZ* amplicons. A uniform temperature cycle was used for qPCR: 10 min at 95°C followed by 40 cycles of 30 s at 95°C, 60 s at 58°C, and 60 s at 72°C.

### 2.5. Group-specific qPCR and reverse transcription qPCR (RT-qPCR) targeting nosZ genes and transcripts in activated sludge samples

Group-specific quantification of the *nosZ* genes and transcripts in the activated sludge samples was performed with the designed primers and probe sets (Table 1) using TaqMan-based qPCR

**Table 1**
The primers/probe sets developed in this study for group-specific quantification of *nosZ* genes

| Targeted group | Primers /Probe | Sequence (5' → 3') | Degeneracy | Coverage | Efficiency (%) |
|---|---|---|---|---|---|
| NosZG1 | NosZG1F | AAG GTN CGB GTN TAC ATG | 48 | 70% | 91.6 |
| | NosZG1R | CSN NCA TYT CCA TGT GCA | 64 | (77/110) | |
| | NosZG1P | FAM-ACT GCM VBT GGT TCT GCC AYG C-MGBNFQ | 36 | | |
| NosZG2 | NosZG2F | GRC ATC WKC MMC GAC AAG | 32 | 84.4% | 93.4 |
| | NosZG2R | HYC TCG RYG TTG TAC TGG | 24 | (27/32) | |
| | NosZG2P | FAM-ACC ACS CGC GTG TTC TGC G-MGBNFQ | 2 | | |
| NosZG3 | NosZG3F | CAY TTT GCW CCD GAY AAT ATT GAA | 24 | 95% | 90.7 |
| | NosZG3R | BSH WGT TTC ACC BGG CAT | 108 | (19/20) | |
| | NosZG3P | FAM-AAY YTR GAA CAA GAY TGG GAT GTA CCK C-MGBNFQ | 32 | | |
| NosZG4 | NosZG4F | ATW GTT GCY GGH GGM AAA | 24 | 57.1% | 94.9 |
| | NosZG4R | TTC CCA DGT KCC DAW TTT | 36 | (4/7) | |
| | NosZG4P | FAM-MGG YGA AGT KSA GAA TCC GGG WT-MGBNFQ | 32 | | |
| NosZG5 | NosZG5F | AAC GAC AAG KCS AAY CCG | 8 | 100% | 97.7 |
| | NosZG5R | GCG GTC GAA CTT CCA GTA | 0 | (5/5) | |
| | NosZG5P | FAM-GCS GTG MTC GAY CTG CGB G-MGBNFQ | 24 | | |

and RT-qPCR assays (FAM as the reporter and NFQ-MGB as the quencher). DNeasy Blood & Tissue Kit (Qiagen) was used to extract DNA from the activated sludge samples. Total RNA was extracted from the methanol-treated samples with RNeasy Mini Kit (Qiagen), purified with DNase I (Qiagen) and RNeasy MinElute Cleanup Kit (Qiagen), and reverse-transcribed with Superscript III (Thermo Fisher Scientific), as described previously (Yoon et al., 2015). The luciferase control mRNA (Promega, Madison, WI, USA) was used as the internal standard to account for RNA loss. Each 20-$\mu$L qPCR mix contained 10 $\mu$L of 2X TaqMan master mix (Applied Biosystems, Foster city, CA, USA), 5 $\mu$M each of forward and reverse primers, 0.5 $\mu$M of probe, and 2 $\mu$L of DNA or cDNA sample. Calibration curves prepared with dilution series of the PCR amplicons were used to calculate the copy numbers of the targeted genes from the $C_t$ values. Eubacterial 16S rRNA genes in the extracted DNA samples were quantified using the 1055F/1392R/Bac115Probe set for estimation of total bacterial population in the activated sludge samples (Table S4). The copy numbers of the targeted *nosZ* genes in the wastewater samples were normalized with the 16S rRNA gene copy numbers for estimation of the relative abundance of the organisms carrying the targeted *nosZ*. For a comparison, the SYBR Green qPCR using the most widely used nosZI and nosZII primers were performed in parallel with the same samples (Table S4).

The PCR amplicons of the Daejeon1 sample amplified with NosZG1-5 primer sets and the NosZI and NosZII primer sets were sequenced using Illumina MiSeq platform (San Diego, CA) at the Center for Health Genomics and Informatics at University of Calgary. The raw sequence reads have been deposited to the SRA database (accession number: PRJNA552418). After quality trimming and merging of the paired-end sequences, the sequences without the probe-binding region were removed, and the remaining reads were clustered into OTUs with 0.97 cut-off using cd-hit-est v4.6 (Li and Godzik, 2006). The OTUs were annotated using blastx search against the bacterial RefSeq database downloaded in June, 2018, with the E-value cut-off and word size set to $10^{-3}$ and 3, respectively, and 'no seg' option selected.

### 2.6. Computational quantification of nosZ genes from shotgun metagenomes of the activated sludge samples

The DNA samples for shotgun metagenome sequencing were extracted with DNeasy PowerSoil Kit (Qiagen) from 50 mL each of the four activated sludge samples analyzed for validation of the qPCR assays. Sequencing of the metagenomic DNA was performed at Macrogen Inc., where HiSeq X Ten sequencing platform (Illumina, San Diego, CA) was used for generating 5-10 Gb of paired-end reads data with 150-bp read length. The raw sequence reads have been deposited to the SRA database (accession numbers: PRJNA552406).

The raw reads were then processed using Trimmomatic v0.36 software with the parameters set to the default values (Bolger et al., 2014). The trimmed reads were translated *in silico* into amino acid sequences using all six possible reading frames and screened for clade I and II *nosZ* sequences using hidden Markov models (HMM). The two HMM algorithms for clade II *nosZ* were downloaded from the Fungene database (accessed in October 2016). As the HMM for clade I *nosZ* in the database had specificity issues, a HMM algorithm was constructed *de novo* using *hmmbuild* command of HMMER v3.1b1 for this clade. The clade I NosZ sequences used to build the HMM were manually curated from the pool of NosZ sequences downloaded from the NCBI database (accessed in October 2016), to represent diverse subgroups within the clade (Table S5) (Hallin et al., 2017; Sanford et al., 2012). The candidate partial NosZ sequences were extracted from the translated shotgun metagenome reads using the *hmmsearch* command of HMMER v3.1b1 with the E-value cut-off set to $10^{-5}$. The nucleotide sequence reads corresponding to the extracted partial NosZ sequences (in separate bins for clade I and clade II NosZ) were assembled into contigs using metaSPAdes v3.12.0 with parameters set to default values (Nurk et al., 2017). The assembled contigs with lengths shorter than 200 bp were filtered out. The overlapping contigs appearing in both clade I and clade II NosZ bins were identified by clustering the two sets of contigs against each other with a nucleotide identity cut-off of 1.0. These overlapping contigs were manually called to the correct bin according to the BLASTX results. The trimmed sequence reads were then mapped onto the contigs in the *nosZ* bins using Bowtie2 v2.2.6, yielding sequence alignments for the contigs and the mapped reads. The alignment files were further processed using samtools v0.1.19, and the PCR duplicates were removed using MarkDuplicates function of picard-tools v1.105 (Li et al., 2009). The sequence coverages of the contigs were calculated using BEDtools v2.17.0 (Quinlan, 2014). The number of reads mapped on to the contigs were normalized with the lengths of the respective contigs. The contigs were assigned taxonomic classification using blastx, and distributed to the NosZG1-5 bins based on their taxonomic affiliations (Table S6). The contigs without matching taxa among those targeted by the NosZG1-5 qPCR were binned as 'other clade I *nosZ* sequences' or 'other clade II *nosZ* sequences'. The attempt to use 16S rRNA sequences extracted with Meta-RNA and assembled with EMIRGE as the template for mapping was not successful, as the coverage of the extracted 16S rRNA sequences turned out to be orders of magnitude lower than the coverages of the single-copy housekeeping genes *rpoB, rpsC, recA, pyrG, lepA*, and *gyrB* computed using the HMM algorithms downloaded from the Fungene database (Huang et al., 2009; Miller et al., 2011). The coverages of the six single-copy housekeeping genes varied by up to five-fold despite the theoretical parity; however, the ratios between the housekeeping genes were constant across the samples (Fig. S3). Thus, the metagenome-derived *nosZ* abundance data were normalized with one of these genes (*rpoB*).

## 3. Results

### 3.1. Active $N_2O$ reducers enriched in fed-batch incubation with varying $N_2O$ concentrations

The microbial communities of the three $N_2O$-reducing enrichments, each prepared with different $N_2O$ concentrations, were analyzed to identify active $N_2O$-reducing groups of microorganisms (Table S7).

Screening for operational taxonomic units (OTUs) with >0.3% abundance in any of the three enrichments yielded 69 OTUs assigned to 33 genera in total, and 14 of these genera were identified with phylogenetic subgroups harboring clade I or clade II *nosZ*. The OTUs belonging to these putatively *nosZ*-harboring genera amounted to 50.8% – 63.2% of the total microbial population in the enrichments. The abundances of the genera putatively harboring clade II *nosZ* were observed to be greater than those of the genera harboring clade I of *nosZ* in all three enrichments (Table S7). In the enrichment incubated with 20 ppmv $N_2O$, *Cloacibacterium* (18.9%), *Flavobacterium* (14.2%), and *Acidovorax* (13.5%) were identified as the dominant genera. *Dechloromonas* (17.3%) and *Flavobacterium* (15.8%) were the dominant genera in the 200-ppmv enrichment, and *Dechloromonas* was the predominant population in the enrichment incubated with 10,000 ppmv of $N_2O$, constituting 46.0% of the total microbial population.

### 3.2. Designing of the degenerate nosZ primers/probe sets

With the 174 translated NosZ sequences affiliated to the 14 genera identified as significant population in the $N_2O$-fed activated sludge enrichments, a phylogenetic tree composed of five distinct branches (NosZG1-5) was constructed (Fig. S4). NosZG1 and NosZG2 were identified as clade I NosZ and NosZG3-NosZG5 as clade II NosZ. The NosZG1, NosZG2, NosZG3, and NosZG5 consisted of 110, 32, 20, and 5 full-length *nosZ* sequences mostly from sequenced genomes or near complete draft genomes. As only a single sequenced genome was available for NosZG4, this group included six putative *Ignavibacterium nosZ* sequences from metagenome-assembled genomes (MAGs). Through an iterative process of designing candidate primers/probe sets and performing *in silico* PCR tests for their evaluation, the degenerate primers/probe sets were developed as to maximize the coverage within the groups while maintaining mutual exclusivity across the groups (Table 1). The *in silico* PCR performed against 174 genomes from which the target *nosZ* sequences were extracted and 50 control genomes without *nosZ* resulted in coverages between 57.3% (NosZG4) and 100% (NosZG5) and complete exclusivity outside their respective target groups (Table 1). The qPCR calibration curves were constructed with the selected model organisms (Fig. S5, Table S8), and despite the high levels of degeneracy (up to 110592), amplification efficiencies above 90% were attained for all five primer and probe sets after optimization.

### 3.3. Evaluation of the group-specific qPCR quantification of nosZ genes

The *nosZ* gene abundances in four distinct activated sludge samples were quantified using the newly designed TaqMan qPCR assays, and the results were compared with those from quantitative analyses of the *nosZ* sequences extracted from the shotgun metagenomes, as well as the results from the SYBR Green qPCR performed with nosZI and nosZII primer sets (Fig. 1, Fig. S6). The TaqMan qPCR results of the four activated sludge samples invariably showed the dominance of the clade II *nosZ* genes (NosZG3 and NosZG5) over clade I *nosZ* genes (NosZG1 and NosZG2) (Fig. 2). In all four activated sludge samples, the sum of the NosZG3 and NosZG5 abundances was no less than five times the sum of NosZG1 and NosG2. The NosZG1-to-NosZG2 and the NosZG3-to-NosZG5 abundance ratios varied by an order of magnitude across the samples. The qPCR targeting the NosZG4 group failed to amplify the clade II *nosZ* belonging to this group. The NosZG4 primers/probe set was designed from a single complete genome (*Ignavibacterium album*) and six sequences from MAGs, which may have been insufficient to cover the sequence divergence of this *nosZ* subgroup.

The distribution of the *nosZ* sequences extracted from the shotgun metagenomes (Table S9) agreed with the TaqMan qPCR results in that the *nosZ* profiles were also severely biased towards the dominance of clade II (Fig. 2, Table S6). The contributions of NosZG1 and NosZG2 to the total *nosZ* gene abundances were minor in all four samples, such that the sum of the relative abundances of NosZG3 and NosZ5 were at least six times larger than the sum of the relative abundances of NosZG1 and NosZG2. The NosZG3-to-NosZG5 abundance ratios were more consistent across the samples (0.67-1.14) than those calculated with the TaqMan qPCR results. The *nosZ* genes sorted as NosZG4 constituted 0.2-1.2% of the total *nosZ* genes grouped as NosZG1-NosZG5, suggesting that this *nosZ* group has less significant role in $N_2O$ reduction in activated sludge tanks than other analyzed groups.

The abundances of clade I *nosZ* in the same activated sludge samples quantified with nosZI SYBR Green qPCR were relatively consistent with the cumulative abundances of NosZG1 and NosZG2 determined with the TaqMan qPCR assays, save for the Daejeon1 sample, where the SYBR Green qPCR yielded 87 times lower copy numbers than the TaqMan qPCR (Fig. S6). The SYBR Green qPCR with the nosZII primer set, with a subpar amplification efficiency of 61.9%, underestimated the clade II *nosZ* copy numbers by several orders of magnitudes, with the largest difference ($1.8\times10^3$-fold) observed with the Daejeon1 sample. The clade I-to-clade II ratios in the activated sludge samples ranged between $6.4 \times 10^{-3}$ to $1.1 \times 10^2$ according to the analyses with the SYBR Green qPCR assays, which contrasted by multiple orders of magnitudes with both the TaqMan qPCR results and the metagenome analyses.

As the qPCR data were normalized with the eubacterial 16S rRNA gene copy numbers and the metagenome-derived relative abundance data were normalized with the sequence coverages of the single-copy housekeeping gene *rpoB*, direct comparisons of the quantitative outcomes of qPCR and metagenome analyses were not possible. It also needs to be stressed that the metagenome-based functional gene quantification is highly reliant on the vol-

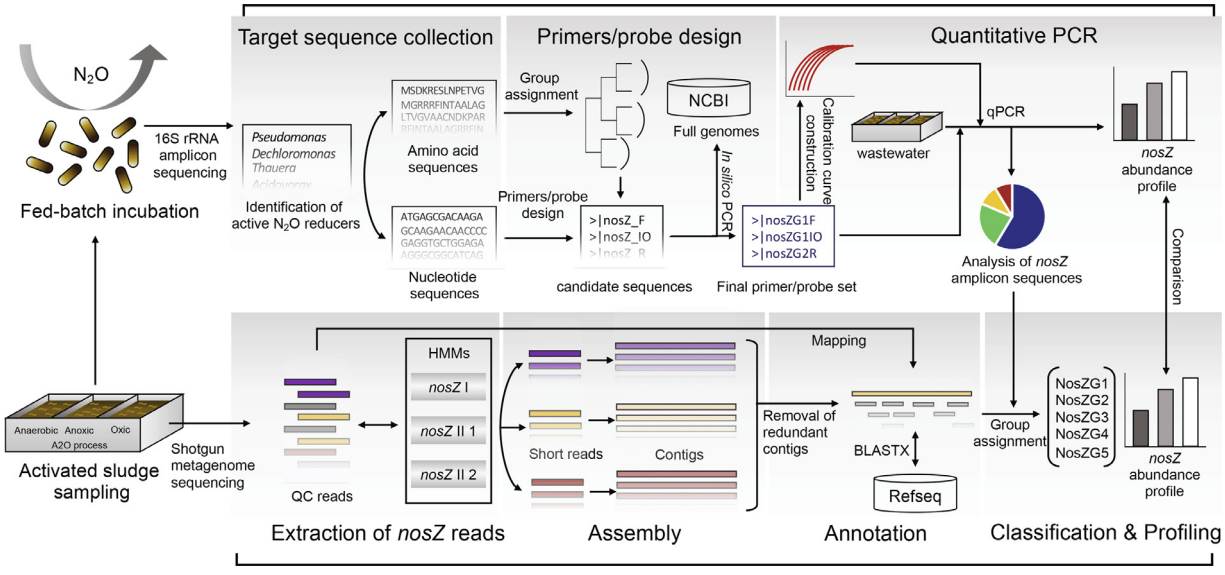


**Fig. 1.** Flow chart for designing of the group-specific *nosZ* primer/probe sets and cross-validation with *nosZ* sequence data extracted from shotgun metagenome data

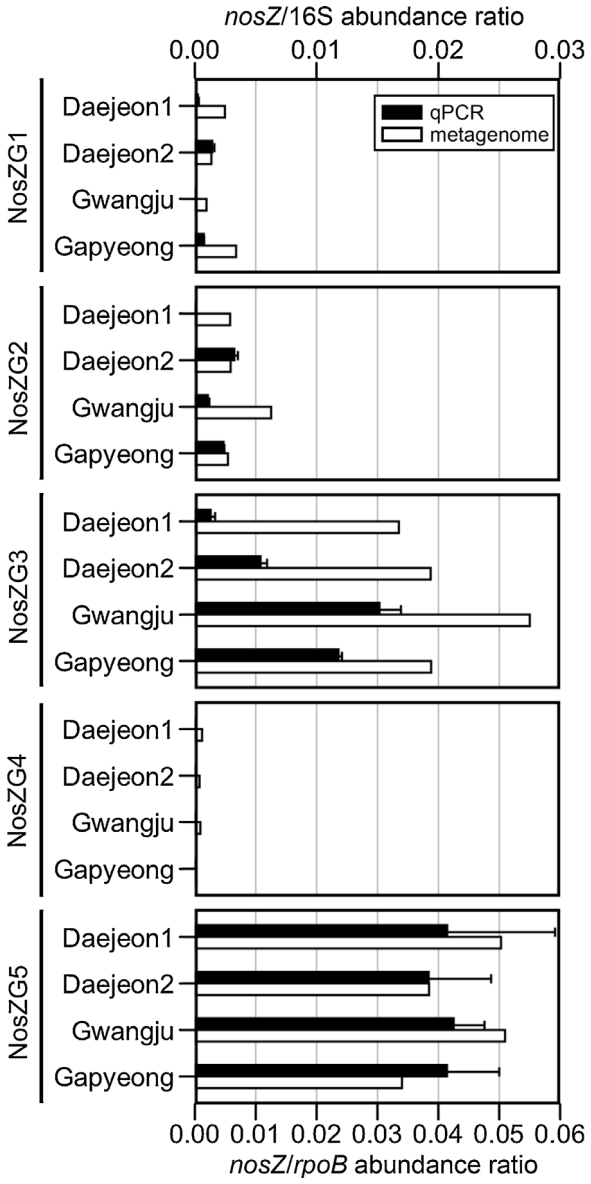


**Fig. 2.** The relative abundances of NosZG1-5 *nosZ* genes as quantified using qPCR and metagenome analysis. The *nosZ* copy numbers from the qPCR assays were normalized with the copy numbers of eubacterial 16S rRNA genes. The coverages of *nosZ* genes in the metagenome data were normalized with the coverages of *rpoB* genes. The presented qPCR quantification data are the averages of triplicate samples processed separately through extraction and qPCR procedures, with the error bars representing their standard deviations.

ume and accuracy of the database and predictability of the algorithms used, and thus, is not a perfect quantitative portrayal of the functional gene profiles. Nevertheless, that the results of the TaqMan qPCR exhibit substantially closer resemblance to those of the metagenome analyses than the results of SYBR Green qPCR is obvious. None of the metagenome analyses returned clade I *nosZ* abundance to be >15% of clade II *nosZ*, while the SYBR Green qPCR results estimated clade I *nosZ* copy numbers >100 greater than clade II *nosZ* copy numbers in two of the four samples analyzed (Fig. S6). The ratio of NosZG1+NosZG2 to the total sum of NosZG1-G5, as measured with the TaqMan qPCR assays, ranged between 1.2% and 7.6%, and remained within the same order of magnitude with the ratio calculated with metagenome analyses. Although the within-clade ratios differed substantially between the TaqMan qPCR and the metagenome analysis, the differences were within an order of magnitude. That the measured copy numbers were orders of magnitudes higher for NosZG3+NosZG5 than clad II *nosZ* quantified with the SYBR-Green qPCR despite of the narrower target groups also clearly indicated higher reliability of the newly designed TaqMan qPCR.

The *nosZ* amplicons of the Daejeon1 sample, amplified with the newly-designed qPCR primer sets as well as the nosZI and nosZII primer sets, were sequenced and analyzed to check whether the qPCR assays were comprehensive and mutually exclusive (Fig. 3). As the NosZG4 primers failed to amplify the targeted genes, NosZG4 was excluded from the analyses. The *nosZ* genes captured by the NosZG1 and NosZG2 primer sets accounted for 54.2% of the entire pool of the clade I *nosZ* genes extracted from the shotgun metagenome. The NosZG3 and NosZG5 primer sets captured 63.4% of the clade II *nosZ* genes extracted from the metagenome (Fig. S7). No amplification outside the targeted group occurred for any of these primer sets, confirming the complete mutual exclusivity of these primers. Each of the qPCR assays were comprehensive within its target groups, as analyzed *nosZ* amplicon sequences covered all genera originally targeted by each primer and probe set. The amplicons from PCR with nosZI and nosZII primer sets covered 61.6% and 85.0% of the clade I and clade II *nosZ* genes extracted from the same metagenome, respectively; however, these amplicons included substantial proportions of non-targeted sequences. The nosZI amplicons included 0.9% and 0.4% of non-*nosZ* and clade II *nosZ* sequences, respectively, and 22.1% of the nosZII amplicons were non-*nosZ* sequences (Fig. S8, Table S6).

Overall, the OTUs identified to be abundant in the PCR amplicons coincided with the dominant *nosZ* OTUs from shotgun metagenome analysis. The OTUs affiliated to *Rhodobacter capsulatus, Rhodobacteraceae* bacterium QY30, *Hyphomicrobium denitrificans*, and *Bradyrhizobium* sp. were the dominant OTUs among the NosZG1 amplicons. The two most abundant *nosZ* OTUs among the NosZG3 amplicons were affiliated to *Flavobacterium columnare* and *Niastella koreensis*, which were also the most abundant *nosZ* taxa according to the metagenome analyses. Subtle discrepancy between the amplicon sequencing data and the shotgun metagenome data were observed for NosZG2 and NosZG5. The OTUs assigned to the genus *Thauera* and *Ruvrivivax gelatinosus* were dominant among NosZG2 amplicons, constituting 50.4% of the amplicons, but together constituted only 2.2% of the metagenome-derived *nosZ* sequences. Instead, an OTU affiliated to *Ramlibacter tataouinensis*, closely related to *R. gelatinosus*, was recovered with high relative abundance (15.4%) in the metagenome-derived NosZG2 pool. Likewise, the low relative abundance of the OTUs affiliated to *Dechloromonas aromatica* (0.2%) among the NosZG5 amplicons was coupled with the high relative abundance of the *nosZ* OTU affiliated to the *Azospira oryzae* (54.6%). The two OTUs shared >96% translated amino acid identity. Thus, the observed discrepancy may have been due to ambiguous NosZ sequence assignments to phylogenetically close OTUs.

### 3.4. Quantitative analyses of nosZ genes and transcripts in activated sludge microbiomes

With the new group-specific *nosZ* primers, the activated sludge microbiomes from anoxic tanks of six additional A2O WWTPs were analyzed for the *nosZ* gene and transcript abundances (Fig. 4). As observed with the samples used for development and validation of the qPCR assays, the clade II *nosZ* (amplified with NosZG3 and NosZG5), were at least three-fold more abundant than the clade I *nosZ* (amplified with NosZG1 and NosZG2) in terms of gene abundance. The *Dechloromonas*-like *nosZ* genes (NosZG5) were the most abundant *nosZ* group in all samples except for the Busan sample, where the abundance of *Flavobacterium*-like *nosZ* genes (NosZG3) was statistically similar to this group. The transcript profiles fur-

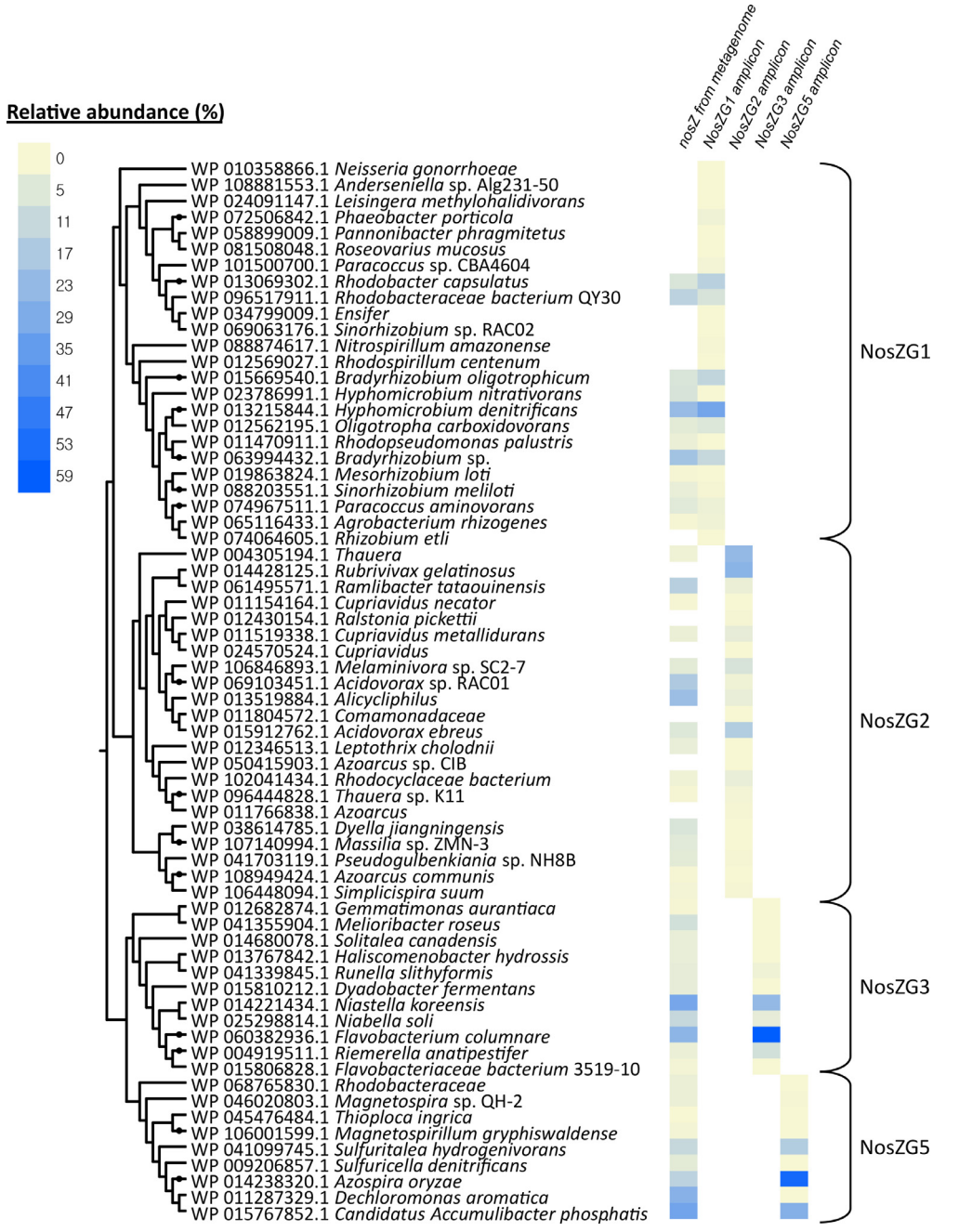


**Fig. 3.** The phylogenetic tree constructed with the reference *nosZ* sequences of the taxa matching OTUs generated from the partial *nosZ* sequences amplified with NosZG1-5 primers. The phylogenetic tree was generated using neighbor-joining method with 500 bootstrap replications. The heatmap shows the relative abundances of the OTUs within each *nosZ* group, computed from the amplicon sequencing data and the *nosZ* sequence data extracted from the metagenome.

ther highlighted the significance of clade II *nosZ* in activated sludge microbiomes. Due to the lower gene abundance and generally low level of transcription observed for clade I *nosZ* (transcript-to-gene ratios lower than 1.0 for both NosZG1 and NosZG2 in five out of six samples), transcription of the clade I *nosZ* was at least an order of magnitude lower than that of the clade II *nosZ* in all activated sludge samples. The *Pseudomonas*-like *nosZ* (NosZG1) had remarkably low transcription level (transcript-to-gene ratios below 0.01) in five out of six samples, suggesting irrelevance of this *nosZ* group as a significant $N_2O$ sink in the activated sludge tanks. The relative importance of NosZG3 and NosZG5 is difficult to fathom, as the *nosZ* transcripts targeted by the NosZG3 primers/probe set were significantly more abundant in the Busan and Gumi sample ($p<0.05$), while the *nosZ* transcripts targeted by NosZG5 primers/probe set were significantly more abundant in the samples from the four other WWTPs ($p<0.05$).

## 4. Discussion

Quantification of the functional genes encoding the nitrogen cycle enzymes (e.g., bacterial/archaeal *amoA*, comammox *amoA, nrfA*, and clade I and II *nosZ*) has been used in increasing number of studies across diverse disciplines of environmental sciences and engineering, as predictors of nitrogen cycling activity in diverse soil and aquatic environments (Chen et al., 2013; Ma et al., 2019; Meinhardt et al., 2015; Pjevac et al., 2017). Despite the frequent use of qPCR in determining the potential $N_2O$-reducing populations, i.e., clade I and clade II *nosZ*-posessing microorganisms, the

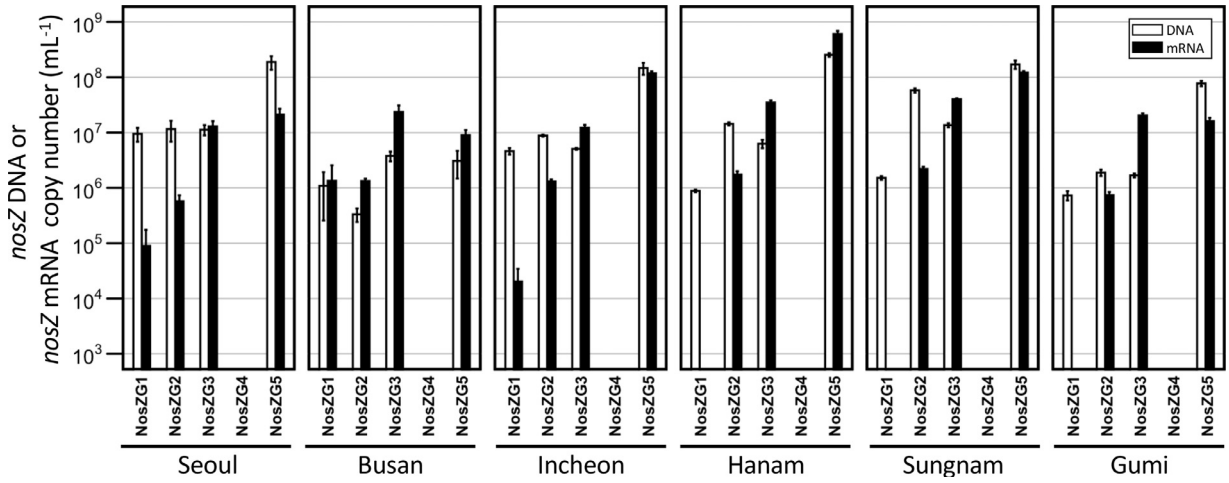


**Fig. 4.** The copy numbers of NosZG1-5 *nosZ* genes and transcripts in activated sludge samples collected from anoxic tanks of six activated sludge-type WWTPs in Korea, as quantified using the group-specific *nosZ* qPCR developed in this study. The presented data are the averages of triplicate samples processed separately through extraction, purification and reverse transcription (for analyses of transcripts), and qPCR procedures, with the error bars representing their standard deviations.

predictability of qPCR quantification has rarely been experimentally scrutinized in the previous studies. The new group-specific qPCR assays exhibited definite advantages over these frequently used primers. (1) Although the targets for primers/probe design were limited to the groups of *nosZ*-possessing organisms enriched with $N_2O$ in *ex situ* cultures, the copy numbers obtained were, in many cases, orders of magnitudes larger than those measured using the nosZI and nosZII primer sets, indicating significantly improved coverage (Fig. S6). (2) The >90% amplification efficiency of the NosZG1-NosZG5 primers/probe sets ensured reliable quantification of the targetted *nosZ* genes and transcripts. (3) Most of the major *nosZ* OTUs (>1% in relative abundance) recovered in metagenome-based *nosZ* profiling of the examined activated sludge samples were amplified with exactly one of the four primer sets, thus confirming the uncompromised coverage and absolute mutual exclusiveness of the primers/probe sets. (4) Subdividing of clade I *nosZ* into NosZG1 and NosZG2 target groups enabled separate quantification of the two subgroups of clade I *nosZ*, which exhibited clearly distinguishable transcription patterns in the anoxic activated sludge samples.

Any methods for quantification of functional genes are prone to error, and the *nosZ* qPCR methods developed here also have certain deficiencies, including inability to amplify *nosZ* genes affiliated to potentially significant *Ignavibacterium* spp. (Fig. 2). Further, a trade-off between coverage (limiting false-negatives) and mutual exclusivity (limiting false-positives) was inevitable and thus, approximately 15 to 50% of the *nosZ* sequences identified in the metagenome were not recovered from the NosG1-5 PCR amplicons (Fig. S7). This apparently incomplete coverage, as well as the subtle discrepancy between the qPCR- and metagenome-based quantification results may as well have resulted from the imperfect nature of metagenomic data processing rather than the qPCR assays themselves (Lindgreen et al., 2016). Thus, comparisons between the qPCR results and metagenomics data in this study need to be received as a mutual validation. In this respect, the results of the three-way comparison with the metagenome analyses and the SYBR Green qPCR assays (Table S6, Fig. S6) are sufficient to support that the qPCR methods developed in this study are, with little doubt, the most quantitatively reliable tools for real-time quantification of *nosZ* genes in wastewater microbiomes, despite their imperfectness.

Some may also criticize reliance of our primers/probe design on the *nosZ* sequences downloaded from the genome database. Theoretically, the approach using *nosZ* sequences extracted from shotgun metagenomes of $N_2O$-enrichment cultures or the activated sludge samples would have been idealistic; however, due to several critical practical issues, we found that such approach is not a feasible option for design of qPCR targeting functional genes with extensive macro- and micro-diversity. *De novo* assembly of short reads is often prone to error, and the mismatches in the primers/probe sets due to the misassembled sequences proved to be critical for qPCR performance in our failed attempts (Murphy et al., 2015). Further, assembly of *nosZ* short reads in the bins yielded mostly partial sequences, which were unsuitable for finding conserved regions for primers/probe design. These issues were aggravated by the small number of short reads assigned to each target *nosZ* group. More recently developed sequencing platforms with substantially longer reads, e.g., single molecule real-time DNA sequencers and nanopore-based sequencers, may be considered as a solution to these short-read related issues; however, their limited throughput and high error rates are critically problematic for the purpose. Therefore, while primer design based on metagenome data may have proved successful when targeting well-conserved genes, e.g., *amoB* of comammox *Nitrospira*, reliance on sequences imported from NCBI RefSeq database was the only viable approach for *nosZ* (Cotto et al., 2020).

The clade II *nosZ*-possessing organisms of the *Flavobacterium* (amplified with NosZG3), *Dechloromonas*, and *Azospira* (amplified with NosZG5) genera have previously been characterized with high-affinity reduction of $N_2O$ (Betlach and Tiedje, 1981; Suenaga et al., 2019; Suenaga et al., 2018; Yoon et al., 2016). The whole-cell half-saturation constants as low as 0.324 $\mu$M has been reported for these groups of $N_2O$ reducers. The *nosZ* gene and transcript pools of all six of the activated sludge samples were dominated by these clade II *nosZ* (targeted by NosZG3 and NosZG5). This observation, along with the high transcript-to-gene ratios support the previous hypothesis that the clade II *nosZ*, with higher affinity to $N_2O$, may have consequential role in suppressing $N_2O$ emissions from anoxic activated sludge tanks (Conthe et al., 2018a; Suenaga et al., 2019). The low transcript-to-gene ratios of the clade I *nosZ* (<0.1 in five out of six samples) targeted by NosZG1 and NosZG2 were also notable in the *nosZ* transcript profiles (Fig. 4). The transcription of NosZG1-targeted *nosZ* was especially low, with $<10^5$ transcripts $mL^{-1}$ (<1% of the transcript copy numbers of *nosZ* affiliated to NosZG3 or NosZG5 groups) in five of six activated sludge samples, indicating $N_2O$ as an unlikely growth substrate for the organisms harboring these *nosZ* genes in the anoxic activated sludge tanks. This observation was in line with the previous bioki-

netic analyses that characterized *Pseudomonas stutzeri* and *Paracoccus denitrificans* harboring *nosZ* genes affiliated to this group with the whole-cell half-satruation constants higher than 30 $\mu$M, an order of magnitude higher than those measured with the organisms harboring clade II *nosZ* (Suenaga et al., 2018; Yoon et al., 2016). Almost exclusively denitrifiers, the organisms harboring these *nosZ* genes may favor upstream steps of denitrification reaction in the anoxic activated sludge tanks, where $NO_3^-$ and/or $NO_2^-$ are constantly available at millimolar concentrations, while dissolved $N_2O$, available in sub-micromolar concentrations, is immediately consumed by their cohabitants equipped with NosZ with substantially higher affinity. Although at substantially lower level than the two clade II *nosZ* groups, *nosZ* belonging to NosZG2 were consistently transcribed across the activated sludge samples (Fig. 4). Along with the observation that *Acidovorax* genus was one of the highly enriched taxa in the fed-batch culture enriched with 20 ppmv $N_2O$ (Table S7), the consistent *nosZ* transcription suggests that this subgroup of clade I *nosZ* may be actively involved in high-affinity $N_2O$ reduction *in situ*, and in that respect, is distinguished from the NosZG1 target group. More physiological evidences are warranted in the future research, however, to verify these hypotheses, as any further extrapolation from the *nosZ* transcription data alone would be an over-interpretation.

The major *nosZ*-possessing organisms identified in the amplicon sequencing and metagenomic analyses differ greatly from the major *nosZ*-possessing populations of the agricultural soils analyzed previously with shotgun metagenome sequencing (Orellana et al., 2014). None of the six most abundant *nosZ* phylogenetic groups in the Havana and Urbana agricultural research site soils (the *nosZ* genes affiliated to *Anaeromyxobacter, Opitutus, Hydrogenobacter, Ignavibacterium, Dyedobacter*, and *Gemmatimonas*, none of which is confirmed denitrifier) was identified as a major population in any of the activated sludge metagenomes examined in this study. Neither were they enriched with $N_2O$ to high relative abundance (e.g., >1%) in the fed-batch reactor at any $N_2O$ concentration applied. *Anaeromyxobacter dehalogenans* and *Gemmatimonas aurentiaca* have been previously confirmed of $N_2O$ reduction activity; however, the $N_2O$ reduction rates measured *in vitro* were orders of magnitudes lower for these organisms than other examined $N_2O$-reducing organisms throughout the entire range of $N_2O$ concentration, and *G. aurantiaca* lacked the capability to utilize $N_2O$ as the growth substrate (Park et al., 2017; Sanford et al., 2012; Yoon et al., 2016). The differences in the compositions of the *nosZ*-possessing populations may thus be attributed to the inherent difference in the rates of the nitrogen turnover processes in WWTP activated sludges and soils. Rapid nitrogen cycling reactions take place on a constant basis in WWTPs, while the time scale of the biogeochemical processes in agricultural soils is orders of magnitude longer and often, nitrogen supply provided through fertilization and plant exudation is sparse and sporadic (Cassman et al., 2002; Law et al., 2012). In fact, incubation of soil microbial consortium with $N_2O$ in the same fed-batch cultivation resulted in enrichment of the same organismal groups as those observed in abundance in the activated sludge samples or enrichments (e.g., *Pseudomonas, Flavobacterium, Acidovorax,* and *Chryseobacterium*) (Table S10). Also notable was that none of quantitatively significant *nosZ* in the wastewater microbiomes belonged to the taxa identified as non-denitrifying $N_2O$ reducers, implying that the abundance of non-denitrifier taxa may not be a reliable predictor of the $N_2O$ sink capability of wastewater microbiomes, as previously proposed.

## 5. Conclusions

This abundance and composition of $N_2O$-reducing organisms are critical determinants for $N_2O$ emissions from WWTP. The qPCR quantification tools for separate quantification of the two clades of *nosZ* have been around for a while; however, generally low PCR efficiencies have been reported for these qPCR, barring reliable comparative quantification of the two *nosZ* clades. Further, there has recently been a growing demand for *nosZ* quantification tools with more specified target groups. Here, five sets of group-specific primers/probe sets, targeting two groups of clade I *nosZ* and three groups of clade II *nosZ* were designed *de novo* for improved quantitative analyses of *nosZ* genes and transcripts in activated sludge. In the validation experiments performed with the DNA extracted from four distinct activated sludge samples, the qPCR assays with the new primer/probe sets (with exception of NosZG4) exclusively and comprehensively amplified their respective target *nosZ* groups, and the quantitative data exhibited much closer resemblance to the metagenome-based *nosZ* quantification than the previous SYBR Green qPCR targeting clade I and clade II *nosZ*. Quantitative analyses of the *nosZ* genes and transcripts in six activated sludge samples using these group-specific primers/probe sets identified the comparative importance of two clade II *nosZ* groups in determining the $N_2O$ sink capability of activated sludge microbiomes. The distinction between the two subgroups of clade I *nosZ*-harboring organisms in terms of their involvement in high-affinity $N_2O$ reduction was also suggested from the *nosZ* transcription profiles obtained with RT-qPCR using these primers/probe sets.

## Declaration of Competing Interest

The authors declare that they have no known competing financial interests or personal relationships that could have appeared to influence the work reported in this paper.

## Acknowledgements

This work was financially supported by “the R&D Center for reduction of Non-CO2 Greenhouse Gases (Grant No. 2017002420002)” funded by Korea Ministry of Environment (MOE).

## Supplementary materials

Supplementary material associated with this article can be found, in the online version, at doi:10.1016/j.watres.2020.116261.

## References

Betlach, M.R., Tiedje, J.M., 1981. Kinetic explanation for accumulation of nitrite, nitric oxide, and nitrous oxide during bacterial denitrification. Appl. Environ. Microbiol. 42 (6), 1074–1084.
Binder, B.J., Liu, Y.C., 1998. Growth rate regulation of rRNA content of a marine *Synechococcus* (Cyanobacterium) strain. Appl. Environ. Microbiol 64 (9), 3346–3351.
Bolger, A.M., Lohse, M., Usadel, B., 2014. Trimmomatic: a flexible trimmer for Illumina sequence data. Bioinformatics 30 (15), 2114–2120.
Boonnorat, J., Techkarnjanaruk, S., Honda, R., Ghimire, A., Angthong, S., Rojviroon, T., Phanwilai, S., 2018. Enhanced micropollutant biodegradation and assessment of nitrous oxide concentration reduction in wastewater treated by acclimatized sludge bioaugmentation. Sci. Tot. Environ. 637-638, 771–779.
Cassman, K.G., Dobermann, A., Walters, D.T., 2002. Agroecosystems, nitrogen-use efficiency, and nitrogen management. Ambio 132-140 (2), 139 31.
Chen, X., Peltier, E., Sturm, B.S.M., Young, C.B., 2013. Nitrogen removal and nitrifying and denitrifying bacteria quantification in a stormwater bioretention system. Water Res. 47 (4), 1691–1700.
Ciais, P., Sabine, C., Bala, G., Bopp, L., Brovkin, V., Canadell, J., Chhabra, A., DeFries, R., Galloway, J., Heimann, M., Jones, C., Le Quere, C., Myneni, R.B., Piao, S., Thornton, P., 2013. Carbon and other biogeochemical cycles. In: Climate Change 2013: The Physical Science Basis. Contribution of Working Group I to the Fifth Assessment Report of the Intergovernmental Panel on Climate Change. Cambridge University Press, Cambridge, United Kingdom, New York, NY, USA, pp. 465–570 Stocker, T. F., Qin, D., Plattner, G.-K., Tignor, M., Allen, S. K., Boschung, J., Nauels, A., Xia, Y., Bex, V., Midgley, P. M., Eds.
Conthe, M., Kuenen, J.G., Kleerebezem, R., van Loosdrecht, M.C.M., 2018. Exploring microbial $N_2O$ reduction: a continuous enrichment in nitrogen free medium. Environ. Microbiol. Rep. 10 (1), 102–107.
Conthe, M., Wittorf, L., Kuenen, J.G., Kleerebezem, R., Hallin, S., van Loosdrecht, M.C.M., 2018a. Growth yield and selection of *nosZ* clade II types in a continuous enrichment culture of $N_2O$ respiring bacteria. Environ. Microbiol. Rep. 10 (3), 239–244.

Conthe, M., Wittorf, L., Kuenen, J.G., Kleerebezem, R., van Loosdrecht, M.C.M., Hallin, S., 2018b. Life on $N_2O$: deciphering the ecophysiology of $N_2O$ respiring bacterial communities in a continuous culture. ISME J. 12 (4), 1142–1153.

Cotto, I., Dai, Z., Huo, L., Anderson, C.L., Vilardi, K.J., Ijaz, U., Khunjar, W., Wilson, C., De Clippeleir, H., Gilmore, K., 2020. Long solids retention times and attached growth phase favor prevalence of comammox bacteria in nitrogen removal systems. Water Res. 169, 115268.

Di, H.J., Cameron, K.C., Podolyan, A., Robinson, A., 2014. Effect of soil moisture status and a nitrification inhibitor, dicyandiamide, on ammonia oxidizer and denitrifier growth and nitrous oxide emissions in a grassland soil. Soil Biol. Biochem. 73, 59–68.

Domeignoz-Horta, L.A., Spor, A., Bru, D., Breuil, M.-C., Bizouard, F., Leonard, J., Philippot, L., 2015. The diversity of the $N_2O$ reducers matters for the $N_2O$:$N_2$ denitrification end-product ratio across an annual and a perennial cropping system. Front. Microbiol. 6, 971.

Edgar, R.C., 2004. MUSCLE: multiple sequence alignment with high accuracy and high throughput. Nucleic Acids Res. 32 (5), 1792–1797.

Frutos, O.D., Quijano, G., Aizpuru, A., Muñoz, R., 2018. A state-of-the-art review on nitrous oxide control from waste treatment and industrial sources. Biotechnol. Adv. 36 (4), 1025–1037.

Gabarró, J., Hernández-del Amo, E., Gich, F., Ruscalleda, M., Balaguer, M.D., Colprim, J., 2013. Nitrous oxide reduction genetic potential from the microbial community of an intermittently aerated partial nitritation SBR treating mature landfill leachate. Water Res. 47 (19), 7066–7077.

Gardner, S.N., Slezak, T.J.B.B., 2014. Simulate_PCR for amplicon prediction and annotation from multiplex, degenerate primers and probes. BMC Bioinform. 15 (1), 237.

Hallin, S., Philippot, L., Löffler, F.E., Sanford, R.A., Jones, C.M., 2017. Genomics and ecology of novel $N_2O$-reducing microorganisms. Trends Microbiol. 26 (1), 43–55.

Henry, S., Bru, D., Stres, B., Hallet, S., Philippot, L., 2006. Quantitative detection of the *nosZ* gene, encoding nitrous oxide reductase, and comparison of the abundances of 16S rRNA, *narG*, *nirK*, and *nosZ* genes in soils. Appl. Environ. Microbiol. 72 (8), 5181–5189.

Huang, Y., Gilna, P., Li, W., 2009. Identification of ribosomal RNA genes in metagenomic fragments. Bioinformatics 25 (10), 1338–1340.

Hysom, D.A., Naraghi-Arani, P., Elsheikh, M., Carrillo, A.C., Williams, P.L., Gardner, S.N., 2012. Skip the alignment: degenerate, multiplex primer and probe design using K-mer matching instead of alignments. PloS One 7 (4), e34560.

Jones, C.M., Spor, A., Brennan, F.P., Breuil, M.-C., Bru, D., Lemanceau, P., Griffiths, B., Hallin, S., Philippot, L., 2014. Recently identified microbial guild mediates soil $N_2O$ sink capacity. Nat. Clim. Change 4, 801–805.

Kumar, S., Stecher, G., Tamura, K., 2016. MEGA7: molecular evolutionary genetics analysis version 7.0 for bigger datasets. Mol. Biol. Evol. 33 (7), 1870–1874.

Law, Y., Ye, L., Pan, Y., Yuan, Z., 2012. Nitrous oxide emissions from wastewater treatment processes. Phil. Trans. R. Soc. B 367 (1593), 1265–1277.

Li, H., Handsaker, B., Wysoker, A., Fennell, T., Ruan, J., Homer, N., Marth, G., Abecasis, G., Durbin, R., 2009. The sequence alignment/map format and SAMtools. Bioinformatics 25 (16), 2078–2079.

Li, W., Godzik, A., 2006. Cd-hit: a fast program for clustering and comparing large sets of protein or nucleotide sequences. Bioinformatics 22 (13), 1658–1659.

Lindgreen, S., Adair, K.L., Gardner, P.P., 2016. An evaluation of the accuracy and speed of metagenome analysis tools. Sci. Rep. 6, 19233.

Ma, Y., Zilles, J.L., Kent, A.D., 2019. An evaluation of primers for detecting denitrifiers via their functional genes. Environ. Microbiol. 21 (4), 1196–1210.

Matsuki, T., Watanabe, K., Fujimoto, J., Miyamoto, Y., Takada, T., Matsumoto, K., Oyaizu, H., Tanaka, R., 2002. Development of 16S rRNA-gene-targeted group-specific primers for the detection and identification of predominant bacteria in human feces. Appl. Environ. Microbiol. 68 (11), 5445–5451.

Meinhardt, K.A., Bertagnolli, A., Pannu, M.W., Strand, S.E., Brown, S.L., Stahl, D.A., 2015. Evaluation of revised polymerase chain reaction primers for more inclusive quantification of ammonia-oxidizing archaea and bacteria. Environ. Microbiol. Rep. 7 (2), 354–363.

Miller, C.S., Baker, B.J., Thomas, B.C., Singer, S.W., Banfield, J.F., 2011. EMIRGE: reconstruction of full-length ribosomal genes from microbial community short read sequencing data. Genome Biol. 12 (5), R44.

Murphy, R.R., O'Connell, J., Cox, A.J., Schulz-Trieglaff, O., 2015. NxRepair: error correction in de novo sequence assembly using Nextera mate pairs. PeerJ 3, e996.

Nurk, S., Meleshko, D., Korobeynikov, A., Pevzner, P.A., 2017. metaSPAdes: a new versatile metagenomic assembler. Genome Res. 27 (5), 824–834.

Orellana, L.H., Rodriguez-R, L.M., Higgins, S., Chee-Sanford, J.C., Sanford, R.A., Ritalahti, K.M., Löffler, F.E., Konstantinidis, K.T., 2014. Detecting nitrous oxide reductase ( *nosZ*) genes in soil metagenomes: method development and implications for the nitrogen cycle. mBio 5 (3), e01114–e01193.

Park, D., Kim, H., Yoon, S., 2017. Nitrous oxide reduction by an obligate aerobic bacterium *Gemmatimonas aurantiaca* strain T-27. Appl. Environ. Microbiol. 72 (4), 2765–2774.

Pjevac, P., Schauberger, C., Poghosyan, L., Herbold, C.W., van Kessel, M.A.H.J., Daebeler, A., Steinberger, M., Jetten, M.S.M., Lücker, S., Wagner, M., Daims, H., 2017. *amoA* -targeted polymerase chain reaction primers for the specific detection and quantification of comammox *Nitrospira* in the environment. Front. Microbiol. 8, 1508.

Portmann, R., Daniel, J., Ravishankara, A., 2012. Stratospheric ozone depletion due to nitrous oxide: influences of other gases. Phil. Trans. R. Soc. B 367 (1593), 1256–1264.

Quinlan, A.R., 2014. BEDTools: the swiss-army tool for genome feature analysis. Curr. Protoc. Bioinform. 47 (1) 11.12.11-11.12.34.

Ravishankara, A., Daniel, J.S., Portmann, R.W., 2009. Nitrous oxide ($N_2O$): the dominant ozone-depleting substance emitted in the 21st century. Science 326 (5949), 123–125.

Ritalahti, K.M., Amos, B.K., Sung, Y., Wu, Q., Koenigsberg, S.S., Löffler, F.E., 2006. Quantitative PCR Targeting 16S rRNA and reductive dehalogenase genes simultaneously monitors multiple *Dehalococcoides* strains. Appl. Environ. Microbiol. 72 (4), 2765–2774.

Sanford, R.A., Wagner, D.D., Wu, Q., Chee-Sanford, J.C., Thomas, S.H., Cruz-García, C., Rodríguez, G., Massol-Deyá, A., Krishnani, K.K., Ritalahti, K.M., Nissen, S., Konstantinidis, K.T., Löffler, F.E., 2012. Unexpected nondenitrifier nitrous oxide reductase gene diversity and abundance in soils. Proc. Natl. Acad. Sci. 109 (48), 19709–19714.

Song, K., Suenaga, T., Harper, W.F., Hori, T., Riya, S., Hosomi, M., Terada, A., 2015. Effects of aeration and internal recycle flow on nitrous oxide emissions from a modified Ludzak–Ettinger process fed with glycerol. Environ. Sci. Pollut. Res. 22 (24), 19562–19570.

Stoliker, D.L., Repert, D.A., Smith, R.L., Song, B., LeBlanc, D.R., McCobb, T.D., Conaway, C.H., Hyun, S.P., Koh, D.-C., Moon, H.S., Kent, D.B., 2016. Hydrologic controls on nitrogen cycling processes and functional gene abundance in sediments of a groundwater flow-through lake. Environ. Sci. Technol. 50 (7), 3649–3657.

Strohm, T.O., Griffin, B., Zumft, W.G., Schink, B., 2007. Growth yields in bacterial denitrification and nitrate ammonification. Appl. Environ. Microbiol. 73 (5), 1420–1424.

Suenaga, T., Hori, T., Riya, S., Hosomi, M., Smets, B.F., Terada, A., 2019. Enrichment, isolation, and characterization of high-affinity $N_2O$-reducing bacteria in a gas-permeable membrane reactor. Environ. Sci. Technol. 53 (20), 12101–12112.

Suenaga, T., Riya, S., Hosomi, M., Terada, A., 2018. Biokinetic characterization and activities of $N_2O$-reducing bacteria in response to various oxygen levels. Front. Microbiol. 9, 697.

Thomson, A.J., Giannopoulos, G., Pretty, J., Baggs, E.M., Richardson, D.J., 2012. Biological sources and sinks of nitrous oxide and strategies to mitigate emissions. Phil. Trans. R. Soc. 367 (1593), 1157–1168.

van den Berg, E.M., Boleij, M., Kuenen, J.G., Kleerebezem, R., van Loosdrecht, M.C.M., 2016. DNRA and denitrification coexist over a broad range of acetate/N-$NO_3^-$ ratios, in a chemostat enrichment culture. Front. Microbiol. 7, 1842.

Vieira, A., Galinha, C.F., Oehmen, A., Carvalho, G., 2019. The link between nitrous oxide emissions, microbial community profile and function from three full-scale WWTPs. Sci. Tot. Environ. 651, 2460–2472.

Wu, L., Ning, D., Zhang, B., Li, Y., Zhang, P., Shan, X., Zhang, Q., Brown, M.R., Li, Z., Van Nostrand, J.D., Ling, F., Xiao, N., Zhang, Y., Vierheilig, J., Wells, G.F., Yang, Y., Deng, Y., Tu, Q., Wang, A., Global Water Microbiome, C., Zhang, T., He, Z., Keller, J., Nielsen, P.H., Alvarez, P.J.J., Criddle, C.S., Wagner, M., Tiedje, J.M., He, Q., Curtis, T.P., Stahl, D.A., Alvarez-Cohen, L., Rittmann, B.E., Wen, X., Zhou, J., 2019. Global diversity and biogeography of bacterial communities in wastewater treatment plants. Nat. Microbiol. 4 (7), 1183–1195.

Yoon, H., Song, M.J., Kim, D.D., Sabba, F., Yoon, S., 2019a. A serial biofiltration system for effective removal of low-concentration nitrous oxide in oxic gas streams: mathematical modeling of reactor performance and experimental validation. Environ. Sci. Technol. 53 (4), 2063–2074.

Yoon, H., Song, M.J., Yoon, S., 2017. Design and feasibility analysis of a self-sustaining biofiltration system for removal of low concentration $N_2O$ emitted from wastewater treatment plants. Environ. Sci. Technol. 51 (18), 10736–10745.

Yoon, S., Cruz-Garcia, C., Sanford, R., Ritalahti, K.M., Loffler, F.E., 2015. Denitrification versus respiratory ammonification: environmental controls of two competing dissimilatory $NO_3^-$/$NO_2^-$ reduction pathways in *Shewanella loihica* strain PV-4. ISME J. 9 (5), 1093–1104.

Yoon, S., Nissen, S., Park, D., Sanford, R.A., Löffler, F.E., 2016. Nitrous oxide reduction kinetics distinguish bacteria harboring clade I versus clade II NosZ. Appl. Environ. Microbiol. 82 (13), 3793–3800.

Yoon, S., Song, B., Phillips, R.L., Chang, J., Song, M.J., 2019b. Ecological and physiological implications of nitrogen oxide reduction pathways on greenhouse gas emissions in agroecosystems. FEMS Microbiol. Ecol. 95 (6) fiz066.

Zumft, W.G., 1997. Cell biology and molecular basis of denitrification. Microbiol. Mol. Biol. Rev. 61 (4), 533–616.